A Differential Variational Inequality Approach for the Simulation of Heterogeneous Materials

Lei Wang[1], **Jungho Lee**[1], **Mihai Anitescu**[1], **Anter El Azab**[2], **Lois Curfman McInnes**[1], **Todd Munson**[1], **Barry Smith**[1]

[1]Mathematics and Computer Science Division, Argonne National Laboratory, Argonne, IL 60439, USA
[2]Florida State University, Tallahassee, FL 32310, USA

Abstract. The phase-field method has recently emerged as a powerful computational approach for modeling and predicting mesoscale morphological and microstructure evolution in materials. While differential variational inequalities (DVIs) arise naturally in the phase-field method, the prevailing approach replaces these by smooth approximations that result in equations that are typically very stiff and limit the efficiency and accuracy of the numerical methods applied. This paper discusses initial work in formulating the phase-field equations as a DVI, which is equivalent to a complementarity problem. We solve the system with newly developed nonlinear algebraic solvers for variational inequalities, and we demonstrate that this DVI approach is accurate and efficient for the resolution of heterogeneous materials problems.

1 Introduction

The interactive evolution of grain boundaries and interfacial networks is a complex process critical to the long-term performance of heterogeneous materials [11]. In this work, we use a phase-field method [5, 10] to model the grain boundaries or interface network. The Center for Materials Science of Nuclear Fuel (CMSNF)[1] is using this approach for modeling microstructure at the mesoscale. The phase-field method is based on expressing the total free energy functional $\mathcal{E}$ of the heterogeneous material in terms of the free energy of each of its constituent phases and interfaces. This functional is used to derive kinetic equations for the conserved field variables $(c_1, c_2, ...)$ and non-conserved phase-field variables $(\eta_1, \eta_2, ...)$ of the system [5]

$$\mathcal{E} = \int f(c_1, c_2, ..., c_n, \eta_1, \eta_2, ..., \eta_p) + \sum_{i=1}^{n} \alpha_i (\nabla c_i)^2 + \sum_{i=1}^{3}\sum_{j=1}^{3}\sum_{k=1}^{p} \beta_{ij} \nabla_i \eta_k \nabla_j \eta_k d^3 r + \int\int G(r - r') d^3 r d^3 r', \tag{1}$$

where f is the local free energy density and α_i and β_i are the gradient energy coefficients. Because the diffuse boundary between phases must be localized, one must use double obstacle potentials for generating the free energy functional. This approach results in a differential variational inequality (DVI). While a comprehensive theory for DVIs has been recently developed [9], the lack of software for large-scale DVIs has led to the situation where the prevailing approach approximates the dynamics of the phase variable by using a smoothed potential. In turn, this (non-DVI) method results in a stiff problem and undesirable physical artifacts: the

[1]CMSNF website: `https://inlportal.inl.gov/portal/server.pt/community/center_for_materials_science_of_nuclear_fuel`

phase-field variable does not have compact support, and the boundary between phases ot grains in the irradiated materials is no longer localized. To circumvent these difficulties, we solve the problem in its natural formulation: as a DVI.

This paper highlights initial results in solving the system by using scalable nonlinear algebraic VI solvers that leverage and extend the capabilities in PETSc [1] and TAO [4], two key libraries of the Towards Optimal Petascale Simulations (TOPS) Center for Enabling Technology.[2]

2 Mathematical Modeling and Discretization

Without loss of generality, we consider a simplified free energy functional

$$\mathcal{E} = \int \left[f(c,\eta) + \frac{\alpha}{2}(\nabla c)^2 + \frac{\beta}{2}(\nabla \eta)^2 \right] d\Omega, \tag{2}$$

where $0 \leq c \leq 1$ is the concentration of a material and $0 \leq \eta \leq 1$ is an order parameter. All analysis can be straightforwardly extended to the general form in (1). Following the standard procedure in the phase-field approach, the kinetic equations for the spatial and temporal evolution of the concentration fields c and the order parameter filed η are the modified Cahn-Hillard equation and Allen-Cahn equations with appropriate boundary conditions,

$$\frac{\partial c}{\partial t} = \nabla \cdot \left(M(c) \nabla \frac{\delta \mathcal{E}}{\delta c} \right) + \xi(\boldsymbol{x}, t), \tag{3}$$

$$\frac{\partial \eta}{\partial t} = -L \frac{\delta \mathcal{E}}{\delta \eta} + \zeta(\boldsymbol{x}, t), \tag{4}$$

where $M(c)$ is the concentration mobility and L is the free surface mobility. The equations hold on the set $0 \leq c \leq 1$ and $0 \leq \eta \leq 1$. The additional terms ξ, ζ in (3) and (4) represent the various sources and sinks for the point defect that exist in a material undergoing irradiation damage. We introduce the chemical potential $w = \frac{\delta \mathcal{E}}{\delta c} = \alpha \Delta c + f_c^{'}(c,\eta)$ and rewrite the fourth-order parabolic equation (3) as a system of equations [3] to obtain

$$\frac{\partial c}{\partial t} = \nabla \cdot (M(c) \nabla w) + \xi(\boldsymbol{x}, t). \tag{5}$$

Unfortunately, a naive finite element approximation of the system (4) and (5) does not a priori guarantee that the discrete solution fulfills $0 \leq c, \eta \leq 1$. Therefore, we impose the physically reasonable property $0 \leq c, \eta \leq 1$ as a constraint. This leads to a variational inequality that must be solved at each time step. Now we consider the finite element approximation of equations (4)-(5) under the following assumptions on the meshes. Let Ω be a polyhedral domain and τ^h be a quasi-uniform family of partitionings of Ω into disjoint open simplices κ with $h_\kappa := \mathrm{diam}(\kappa)$ and $h := \max_{\kappa \in \tau^h} \mathrm{h}_\kappa$, so that $\bar{\Omega} = \cup_{\kappa \in \tau^h} \bar{\kappa}$. Associated with τ^h is the finite element space $S^h := \left\{ \chi \in C\left(\bar{\Omega}\right) : \chi|_\kappa \text{ is linear } \forall \kappa \in \tau^{\mathrm{h}} \right\}, K^h := \left\{ \chi \in S^h : -1 \leq \chi \leq 1 \text{in } \Omega \right\}$. The finite element

[2] TOPS website: `http://www.scalablesolvers.org`

approximation of equations (4)-(5) is as follows: for $n \geq 1$, find $\boldsymbol{c}^n, \boldsymbol{w}^n, \boldsymbol{\eta}^n \in K^h \times S^h \times K^h$

$$\left(\frac{\boldsymbol{c}^n - \boldsymbol{c}^{n-1}}{\Delta t}, \chi_1\right) + (M(c^*)\nabla \boldsymbol{w}^n, \nabla \chi_1) + (\boldsymbol{\xi}^*, \chi_1) = 0, \quad \forall \chi_1 \in S^h,$$

$$\alpha\left(\nabla \boldsymbol{c}^n, \nabla(\chi_2 - \boldsymbol{c}^n)\right) + (f_c^{'}(\boldsymbol{c}^*, \boldsymbol{\eta}^*), \chi_2 - \boldsymbol{c}^n) \geq (\boldsymbol{w}^n, \chi_2 - \boldsymbol{c}^n), \quad \forall \chi_2 \in K^h,$$

$$\left(\frac{\boldsymbol{\eta}^n - \boldsymbol{\eta}^{n-1}}{\Delta t}, \chi_3 - \boldsymbol{\eta}^n\right) + L\left(\beta \nabla \boldsymbol{\eta}^n, \nabla(\chi_3 - \boldsymbol{\eta}^n)\right) + L(f_\eta^{'}(\boldsymbol{c}^*, \boldsymbol{\eta}^*), \chi_3 - \boldsymbol{\eta}^n) + (\boldsymbol{\zeta}^*, \chi_3) \geq 0,$$
$$\forall \chi_3 \in K^h,$$

where $(\cdot)^* = (\cdot)^n$ or $(\cdot)^{n-1}$ and $\boldsymbol{c} = \sum_{i=1}^N c(x_i)\phi_i, \boldsymbol{w} = \sum_{i=1}^N w(x_i)\phi_i, \boldsymbol{\eta} = \sum_{i=1}^N \eta(x_i)\phi_i$ are finite dimension approximations with $\{\phi\}_{i=1}^N$ being the standard Lagrange "hat" basis functions. We have a complementarity formulation [6] of the coupled Cahn-Hillard equation and Allen-Cahn equation (4)-(5):

$$0 = M_0 \frac{\boldsymbol{c}^n - \boldsymbol{c}^{n-1}}{\Delta t} + M_1 \boldsymbol{w}^n + M_0 \boldsymbol{\xi}^*, \tag{6}$$

$$0 = \alpha M_2 \boldsymbol{c}^n + M_0 f_c^{'}(\boldsymbol{c}^*, \boldsymbol{\eta}^*) - M_0 \boldsymbol{\omega}^n + \boldsymbol{\lambda}_1 - \boldsymbol{\mu}_1 \tag{7}$$

$$0 = M_0 \frac{\boldsymbol{\eta}^n - \boldsymbol{\eta}^{n-1}}{\Delta t} + L\beta M_2 \boldsymbol{\eta}^n + L M_0 f_\eta^{'}(\boldsymbol{c}^*, \boldsymbol{\eta}^*) + M_0 \boldsymbol{\zeta}^* + \boldsymbol{\lambda}_2 - \boldsymbol{\mu}_2 \tag{8}$$

$$0 \leq \boldsymbol{\lambda}_1 \perp 1 - \boldsymbol{c}^n \geq 0, \quad 0 \leq \boldsymbol{\mu}_1 \perp \boldsymbol{c}^n \geq 0, \tag{9}$$

$$0 \leq \boldsymbol{\lambda}_2 \perp 1 - \boldsymbol{\eta}^n \geq 0, \quad 0 \leq \boldsymbol{\mu}_2 \perp \boldsymbol{\eta}^n \geq 0, \tag{10}$$

where $M_{0i,j} = (\phi_i, 1)_{L^2(\Omega)}$, $M_{1i,j} = (M(c^*(x_i))\nabla\phi_i, \nabla\phi_j)_{L^2(\Omega)}$ and $M_{2i,j} = (\nabla\phi_i, \nabla\phi_j)_{L^2(\Omega)}$ and $\boldsymbol{\lambda}_{1,2}, \boldsymbol{\mu}_{1,2} \in \mathbb{R}^N$ are Lagrange multipliers. Then we can use parallel matrix-free solvers for complementarity problems in PETSc and TAO.

3 Algorithms and Software

To solve the algebraic DVIs that arise at each timestep of these mesoscale simulations, we are investigating algorithms developed by the optimization community for solving complementary problems based on a formulating them as nonsmooth systems of equations. We have already implemented two parallel nonlinear algebraic VI solvers in the PETSc library: a semi-smooth algorithm and a reduced-space active set algorithm. To solve the resulting linear systems, we are exploring a multigrid method with block Gauss-Seidel smoothing [2] and Schur complement preconditioners that incorporate a multigrid (either algebraic or geometric) solver.

We have completed preliminary numerical experiments and mathematical analysis for the Allen-Cahn system that demonstrate mesh-independent convergence rates for the Schur complement preconditioner. That is, the work required to solve a single timestep grows linearly with the number of unknowns. In Figure 1 we plot the time to solution for 200 timesteps using several solver approaches for the Allen-Cahn model in two dimensions. For the innermost solve in the Schur complement we leverage complementary TOPS capabilities by employing PETSc's interface to LLNL's BoomerAMG algebraic multigrid solver in the hypre library.

4 Numerical Experiments

Here we suppose a polycrystalline metal consisting of two possible stable phases, namely, a matrix phase containing a finite (low) concentration of point defects (vacancies c_v and interstitials

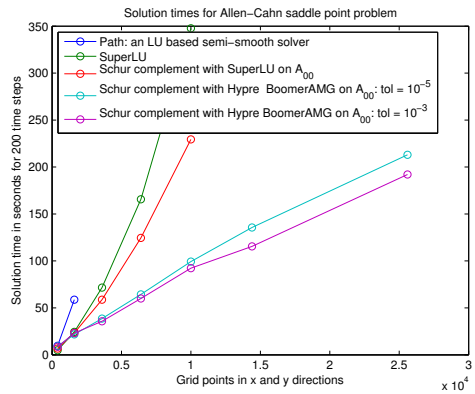

Figure 1: Solution times for an Allen-Cahn saddle point problem; we demonstrate mesh-independent convergence rates for the Schur complement preconditioner that incorporate algebraic multigrid.

c_i) and a void phase defined as a vacancy clusters. This model is introduced in [7]. We omit the detailed description here because of limited space.

Some preliminary computational results are shown in Figure 2. The upper row is the cases of void growth in a supersaturated vacancy field. The void grows as a result of the absorption of vacancies from the adjacent solid regions. The interstitial concentration in the solid remains at equilibrium throughout time. Within the void, the values of the concentration and order parameter fields are $c_v = 1, c_i = 0$ throughout the evolution. The lower row is the void shrinks that occur as a result of the recombination of interstitials with vacancies at the void surface. These numerical results agree with those presented in [7]. One of the benefits of our DVI approach is that the numerical solution c_v and η is in the interval $[0, 1]$ naturally and does not need any clamping.

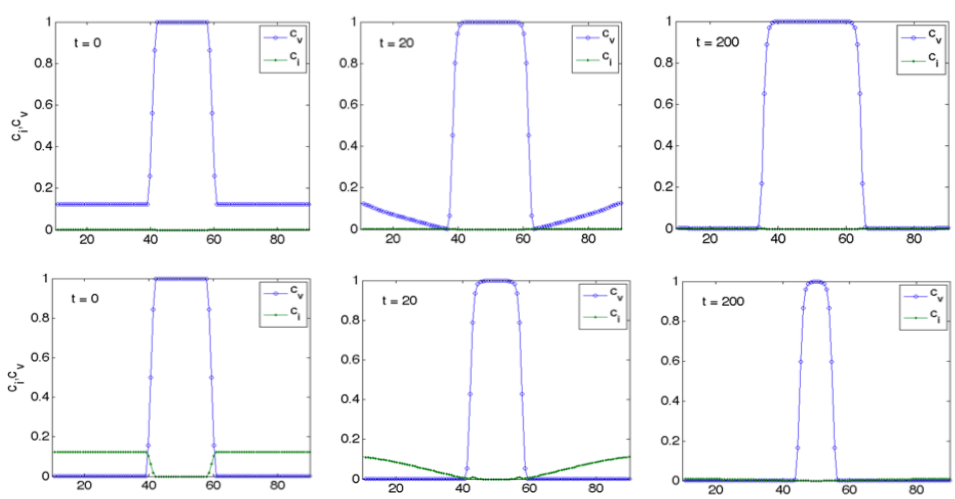

Figure 2: Plots of the concentration fields c_v and c_i through time. Upper row: the void grows due to the absorption of vacancies from the adjacent solid regions. Lower row: the void shrinks due to the recombination of interstitials with vacancies at the void surface.

5 Summary

We use the coupled Cahn-Hilliard and Allen-Cahn systems with a double-obstacle free energy potential to simulate the physics. A naive finite element approximation does not guarantee that the discrete solution satisfies appropriate constraints. Therefore, we formulate a DVI, which is equivalent to a complementarity problem. This approach allows us to use parallel matrix-free solvers for complementarity problems in PETSc and TAO. We have validated the DVI approach against the baseline results of the CMSNF, as provided by Millett et al. in [7], and are extending to address additional models discussed in [8] and high dimensions.

Acknowledgments. This work was supported by the Office of Advanced Scientific Computing Research, Office of Science, U.S. Department of Energy, under Contract DE-AC02-06CH11357.

References

[1] S. Balay, K. Buschelman, V. Eijkhout, W. Gropp, D. Kaushik, M. Knepley, L. McInnes, B. Smith, and H. Zhang, "PETSc Users Manual," Tech. Rep. ANL-95-11-Revision 3.1, Argonne National Laboratory, 2010, see `http://www.mcs.anl.gov/petsc`.

[2] L. Baňas and R. Nürnberg, "A Multigrid Method for the Cahn-Hilliard Equation with Obstacle Potential," Applied Mathematics and Computation (213), no. 2, pp. 290–303, 2009.

[3] J. Barrett, J. Blowey and H. Garcke, "Finite Element Approximation of the Cahn-Hillard Equation with Degenerate Mobility," SIAM J. Numer. Anal. (37), pp. 286-318, 1999.

[4] S. Benson, L. C. McInnes, J. Moré, T. Munson, and J. Sarich, "Toolkit for Advanced Optimization (TAO) Users Manual," Tech. Rep. ANL/MCS-TM242 - Revision 1.10.1, Argonne National Laboratory, 2010, see `http://www.mcs.anl.gov/tao`.

[5] L. Chen, "Phase-field Models for Microstructure Evolution," Annual Review of Materials Research (32), pp. 113-140, 2002.

[6] D. Kinderlehrer and G. Stampacchia, *An Introduction to Variational Inequalities and Their Applications*, Philadelphia: Society for Industrial Mathematics, 2000.

[7] P. Millett, A. EI-Azab, S. Rokkam, M. Tonks and D. Wolf, "Phase-field Simulation of Irradiated Metals, Part I: Void Kinetics," Comp. Mate. Sci. (50), pp. 949–959, 2011.

[8] P. Millett, A. EI-Azab and D. Wolf, "Phase-field Simulation of Irradiated Metals, Part II: Gas Bubble Kinetics," Comp. Mate. Sci. (50), pp. 960–970, 2011.

[9] J.-S. Pang and D. E. Stewart, "Differential Variational Inequalities," Mathematical Programming, (113), no. 2, pp. 345-424, 2008.

[10] K. Thornton, J. Agren and P. Voorhees, "Modeling the Evolution of Phase Boundaries in Solids at the Meso- and Nano-scales," Annual Review of Materials Research (32), pp. 113-140, 2002.

[11] S. Yip, *Handbook of Materials Modeling*, Springer, 2005.